


Hypoxia-induced pulmonary hypertension upregulates eNOS and TGF- β contributing to sex-linked differences in *BMPR2*^{+/R899X} mutant mice

Ejehi O. Erewele¹ | Maricela Castellon^{1,2} | Omar Loya¹ | Glenn Marshboom³ | Andrew Schwartz¹ | Kayla Yerlioglu¹ | Christopher Callahan¹ | Jiwang Chen^{2,4} | Richard D. Minshall^{1,3} | Suellen D. Oliveira^{1,5} 

¹Department of Anesthesiology, College of Medicine, University of Illinois at Chicago, Chicago, Illinois, USA

²Cardiovascular Research Center, College of Medicine, University of Illinois at Chicago, Chicago, Illinois, USA

³Department of Pharmacology and Regenerative Medicine, College of Medicine, University of Illinois at Chicago, Chicago, Illinois, USA

⁴Department of Medicine, College of Medicine, University of Illinois at Chicago, Chicago, Illinois, USA

⁵Department of Physiology & Biophysics, College of Medicine, University of Illinois at Chicago, Chicago, Illinois, USA

Correspondence

Suellen D. Oliveira, Department of Anesthesiology, College of Medicine, University of Illinois at Chicago, 835S. Wolcott Ave., E713 MSB (M/C 515), Chicago, IL 60612, USA; Richard D. Minshall, Department of Pharmacology, College of Medicine, University of Illinois at Chicago, 835S. Wolcott Ave., E709C MSB (M/C 868), Chicago, IL 60612, USA. Email: suelleno@uic.edu

Funding information

American Lung Association, Grant/Award Number: CA697907; National Heart, Lung, and Blood Institute, Grant/Award Numbers: NIH HL142636, NIH HL159037; U.S. Department Education (ED HSI STEM - Loya, O fellowship), Grant/Award Number: P031C160237

Abstract

Dysfunctional bone morphogenetic protein receptor 2 (BMPR2) and endothelial nitric oxide synthase (eNOS) have been largely implicated in the pathogenesis of pulmonary arterial hypertension (PAH); a life-threatening cardiopulmonary disease. Although the incident of PAH is about three times higher in females, males with PAH usually have a worse prognosis, which seems to be dependent on estrogen-associated cardiac and vascular protection. Here, we evaluated whether hypoxia-induced pulmonary hypertension (PH) in humanized *BMPR2*^{+/R899X} loss-of-function mutant mice contributes to sex-associated differences observed in PAH by altering eNOS expression and inducing expansion of hyperactivated TGF- β -producing pulmonary myofibroblasts. To test this hypothesis, male and female wild-type (WT) and *BMPR2*^{+/R899X} mutant mice were kept under hypoxic or normoxic conditions for 4 weeks, and then right ventricular systolic pressure (RVSP) and right ventricular hypertrophy (RVH) were measured. Chronic hypoxia exposure elevated RVSP, inducing RVH in both groups, with a greater effect in *BMPR2*^{+/R899X} female mice. Lung histology revealed no differences in vessel thickness/area between sexes, suggesting RVSP differences in this model are unlikely to be in response to sex-dependent vascular narrowing. On the other

Disclosures: This work was in part presented at 2022 Vascular Biology: From Genes to Medicine (Seattle, WA); at the 2021 University of Illinois College of Medicine (UIC COM) Research Day; at the 2021 UIC Cardiovascular Research Forum (CCVR; Honorable mention by Ejehi O. Erewele); and at the 2022 UIC CCVR (Omar Loya).

This is an open access article under the terms of the Creative Commons Attribution-NonCommercial License, which permits use, distribution and reproduction in any medium, provided the original work is properly cited and is not used for commercial purposes.

© 2022 The Authors. *Pulmonary Circulation* published by John Wiley & Sons Ltd on behalf of Pulmonary Vascular Research Institute.

hand, hypoxia exposure increased vascular collagen deposition, the number of TGF- β -associated α -SMA-positive microvessels, and eNOS expression, whereas it also reduced caveolin-1 expression in the lungs of *BMPR2*^{+/R899X} females compared to males. Taken together, this brief report reveals elevated myofibroblast-derived TGF- β and eNOS-derived oxidants contribute to pulmonary microvascular muscularization and sex-linked differences in incidence, severity, and outcome of PAH.

KEYWORDS

BMPR2, eNOS, pulmonary arterial hypertension, sex-linked differences, TGF- β

INTRODUCTION

Mutations or reduced expression of bone morphogenetic protein receptor 2 (BMPR2) is a hallmark in the onset and development of different subgroups of pulmonary arterial hypertension (PAH), accounting for up to 75% of inherited PAH cases and 11%–40% of idiopathic PAH patients.¹ Although PAH has a clear multifactorial component, lung endothelial cell (EC) injury and expansion of pathogenic cell populations within the pulmonary vascular wall are major triggers of progressive remodeling and narrowing of small pulmonary arteries, characteristic of the disease.^{2,3} In response to increased pulmonary vascular resistance, the pressure inside the right ventricle increases, which often results in right ventricular hypertrophy (RVH) and premature death by heart failure.^{4,5} Despite extensive efforts to alleviate PAH morbidity and reduce its mortality, the disease remains incurable.

Reduced BMPR2-mediated signaling in pulmonary vascular cells is known to contribute to hyperactivation of the TGF- β pathway by shifting endothelial protective P-SMAD1/5/8 signaling to the pathological P-SMAD2/3 pathway. This switch has been reported to significantly contribute to smooth muscle cell, endothelial cell, and fibroblast migratory and proliferative changes characteristic of the disease.^{6,7} It is evident that TGF- β is the major promoter of endothelial-to-mesenchymal transition (EndoMT) in human and animal models, meaning TGF- β leads to the expansion of abnormal EC-derived populations with myofibroblast-like characteristics.⁸ Moreover, loss of endothelial BMPR2 expression is associated with dysfunction of the endothelial protective enzyme, endothelial nitric oxide synthase (eNOS).⁹ Dysfunction or “uncoupling” of eNOS leads to formation of free radical oxidants that perpetuate EC injury as well as contribute to elevated vasoconstriction.^{9,10} Thus, it is evident that balance between BMPR2 and TGF- β -mediated signaling is critical for vascular homeostasis and injury repair.

Imbalance can lead to enhanced TGF- β control over cell phenotype as well as survival, proliferation, and migration mechanisms of the various cell types in the pulmonary vascular wall, including pulmonary ECs.

Of note, over 300 BMPR2 mutations have been identified^{11,12} with the heterozygous nonsense mutation *Bmpr2*R899X in exon 12, inducing age-associated pulmonary hypertension (PH) in mice.¹³ Importantly, amongst the population of heritable PAH patients carrying the heterozygous BMPR2 mutation, males often have a worse prognosis, despite the fact that females have nearly three times higher incidence of this disease.¹⁴ In line with these observations, previous studies indicated that estrogen could reduce BMPR2 expression, thus contributing to the higher prevalence of PAH in females carrying the BMPR2 mutation.^{15–18} Although previous studies have demonstrated that sex plays a role in the prevalence and mortality associated with PAH, the specific mechanism and a selective molecular target behind these sex-associated differences remain under investigation. Together, these observations prompted us to investigate the contribution of lung EC BMPR2 expression and mutation in PAH-associated sexual disparity. In particular, we evaluated whether chronic hypoxia-induced PH in the humanized mouse model carrying the *BMPR2*^{+/R899X} loss-of-function mutation would play a role in the onset of endothelial dysfunction, EndoMT, and pulmonary microvascular muscularization that leads to elevated right ventricular systolic pressure (RVSP) and PAH.

MATERIALS AND METHODS

Mouse model and genotyping

Male and female wildtype (WT) mice and a mutant strain carrying the heterogenous human knock-in mutation *BMPR2*^{+/R899X} were genotyped using amplification

refractory mutation system PCR (ARMS-modified PCR) and the following primers: GAGGGAACGG CCATTA-GAAGGTGGAT (ARMS_mBMP2_inFw); AGAAGC-CACAATGTTAATTCCCATGCTG (ARMS_mBMP2_outFw) and; ATACTGCTGCCATCCAGGATAT TTGTGG (ARMS_mBMP2_outv), as previously described.¹⁹ WT and *BMP2*^{+/*R899X*} mutant mice were randomized by sex for subsequent experiments. In all cases, strain- and age-matched mice were used as approved by the University of Illinois at Chicago Institutional Animal Care and Use Committee.

Hypoxia-induced pulmonary hypertension and hemodynamics assessment

WT and *BMP2*^{+/*R899X*} mutant mice (12-month-old) were randomized and kept under normoxia (21% O₂) or hypoxia chamber (10% O₂) for 4 weeks with water and food access ad libitum. Animals were then weighted and anesthetized using an intraperitoneal injection of Ketamine/Xylazine (100 and 10 mg/kg, respectively). After animals undergo general anesthesia, the surgical area was disinfected using 70% alcohol and a small skin incision was performed to access the jugular vein. As described previously,²⁰ a Millar Mikro-Tip catheter transducer (model PVR-1030) was carefully inserted into the right ventricle (RV) via the right jugular vein for measurement of RVSP, calculated using an MPVS-300 system connected to a Powerlab A/D converter (AD Instruments, Colorado Springs, CO). After recordings were completed, the animals were ventilated, and about 1 ml of blood was collected using 3.8% sodium citrate-treated syringes via vena cava puncture. Then, animals were exsanguinated and lungs were cleared by perfusion of 5 ml of cold PBS via cannula placed in the RV. After complete lung perfusion, the lung lobes were either removed and snap-frozen in liquid nitrogen for Western blot analysis analysis, freshly removed for fibroblast isolation, or carefully inflated with 4% paraformaldehyde (PFA) solution for posterior paraffinization, sectioning, histological and immunohistochemistry analysis. Finally, freshly isolated hearts were dissected for evaluation of RV hypertrophy using the Fulton index (RV/left ventricle + septum weight ratio).²⁰

Lung sample preparation and Western blot analysis

Frozen lung tissue was fully homogenized using cold radiomunoprecipitation assay (RIPA) buffer containing 1% protease and 0.1% phosphatase inhibitor cocktail.

After 20 min incubation at 4°C, homogenates were centrifuged at 12,000×g (20 min at 4°C) and supernatants collected for protein measurement by bicinchoninic acid (BCA) protein assay by colorimetry using a microplate reader (Benchmark Scientific MR9600-T SmartReader™ 96 Plate). Then, 10–20 µg of lung tissue lysates diluted in Laemmli Sample Buffer (4×) with β-mercaptoethanol, boiled by 10 min at 95°C or kept unboiled for native protein analysis to assess eNOS uncoupling by increase in monomers. Before loading the samples on gradient SDS-PAGE gels (8%–12%), tubes were centrifuged for 2.5 min at 16,200×g. After running the samples, separated proteins were transferred to nitrocellulose membranes as described.²¹ Protein transfer to the membranes was assessed by absence of ladder markers in the gel simultaneously with detection of a continuous gradient of Ponceau Rouge staining over the membranes. Membranes were then washed twice with TBS-Tween 1X for 5 min and blocked using 5% milk or BSA (according to antibody datasheet instructions) for 1 h at room temperature, followed by primary antibody incubation overnight at 4°C or 2–3 h at 37°C. After washing (2 × 5 min; 1 × 15 min), the membranes were incubated for 1 h with the specific secondary HRP-conjugated antibody, washed again, and then, proteins were detected using an ECL kit (Amersham). Finally, membranes were scanned with Li-Cor Odyssey CLx (Lincoln, NE). Data were normalized to β-actin or GAPDH loading controls and analyzed using ImageJ software (<https://imagej.nih.gov/ij/>).

Fibroblast isolation, immunostaining, and proliferation assay

Freshly isolated, and perfused lungs from anesthetized mice were excised, and finely minced into 2- to 5-mm fragments, rinsed with sterile PBS, and incubated in 2 mg/ml type I collagenase in DMEM (60 min at 37°C under agitation [≈80 rpm]). After fragments were dissociated and the resulting suspension was filtered through a 40 µm cell strainer, cell suspension was centrifugated (300×g; 8 min), resuspended, and assayed for viability using Trypan blue reagent (2–4 × 10⁶ cells per adult lung). Then, cells were allowed to attach at 37°C on 10 cm tissue culture dishes. After 1 h, nonadherent cells were removed by a gentle washing and remaining attached cells were further cultured in DMEM+ 10% FBS. WT and mutant-derived fibroblasts were cultured under the same conditions. Cell growth was evaluated daily by brightfield microscopy for 7 days, when cells were fixed in 4% PFA solution for 15 min at room temperature.²² After permeabilization, cells were blocked

with 10% donkey or goat serum diluted in PBS for 1 h (room temperature), followed by overnight incubation with primary antibody against Ki67 at 4°C (in a humidified chamber). After washing, slides were incubated with Alexa 488 and Alexa 555 secondary antibodies (excitation/emission: 499/519 and 553/568 nm, respectively) for 1 h, washed again, and mounted on Prolong antifade mounting media containing DAPI (4',6-diamidino-2-phenylindole) for nuclear staining. Cell culture purity was assessed by HSP47 and prolyl 4-hydroxylase staining. Ki67 and DAPI were used to quantify proliferation. Fluorescent images were collected using a confocal microscope (Zeiss LSM810).

Immunohistochemistry and quantification of vascular remodeling

Formalin-fixed, paraffin-embedded lung sections were used to evaluate protein expression (primary antibodies: α -SMA, vWF, and FSP-1) and for histological analysis of vessel area, thickness, and collagen deposition. Samples were deparaffinized by serial exposure to xylene and ethanol and then to high temperature, used to promote antigen retrieval (5–10 min under pressurized container; sodium citrate buffer). For immunohistochemistry, lung sections were blocked using 10% donkey or goat serum diluted in PBS for 1 h (room temperature) followed by overnight incubation with the primary antibody at 4°C (in a humidified chamber). After washing, slides were incubated with antibodies Alexa fluor-labeled secondary antibodies, washed again and mounted and imaged as above. Then, fluorescent images were collected using a LSM880 confocal microscope from Carl Zeiss MicroImaging, Inc. Four fluorescent images were taken from different randomized peripheral lung segments in each sample for manual quantification of alpha-smooth muscle actin (α -SMA) and DAPI expressing muscularized vessels in WT and *BMPR2*^{+/*R899X*} mutant males compared to females. The number of vessels were normalized by the total area. In addition, histological analysis of collagen deposition was performed using picosirius FAST red stained lung sections. After staining, individual slides containing 2–3 lung sections of 5–10 μ m each, were scanned using an Aperio brightfield automated microscope slide scanner (Leica Aperio AT2) at 20x magnification. Digitized images were used to determine the pulmonary microvessel area and thickness (μ m) in 10 microvessels per animal, that is, vessels with a diameter smaller than 100 μ m, specifically varying between 30 and 70 μ m, using the ImageScope software 12.4.6 (Leica Biosystems). Briefly, microvessel wall thickness was obtained via utilization of the ImageScope

ruler tool to measure the length across the thickest part of the arterial segment defined as the space between the peripheral outer wall of the vasculature and luminal boundary. Microvessel wall area was subsequently collected by manually tracing the contours of the peripheral outer wall and luminal boundary to obtain the total microvessel area and luminal area respectively and calculated by subtracting the luminal area from the total area of the microvessel as previously reported.²⁰ Mean microvessel wall thickness and area were calculated for each sample using Excel software.

Enzyme-linked immunosorbent assay (ELISA)

Frozen lung tissue was fully homogenized using cold RIPA buffer containing 1% protease and 0.1% phosphatase inhibitor cocktail. After 20 min incubation at 4°C, tissue homogenates were centrifuged at 12,000 \times g (20 min at 4°C), and the supernatant collected for measurement of interleukin-6 (IL-6) and transforming growth factor- β 1 (TGF- β 1) in male and female WT and *BMPR2*^{+/*R899X*} mutant mice and isolated fibroblasts according to manufacturer instructions (R&D ELISA kits).

Reagents and antibodies

Rabbit polyclonal anti- α -SMA was acquired from Abcam. Rabbit polyclonal anti-GAPDH, anti-von Willebrand Factor (vWF), and anti-fibroblast-specific protein 1 (FSP1) were acquired from Santa Cruz Biotechnology. Rabbit Polyclonal Endothelin-1 was purchased from Fisher Scientific. Rabbit polyclonal anti-BMPRII and anti-P-SMAD1/5/8 were purchased from Cell Signaling Technology. Mouse monoclonal anti-eNOS, anti- β -actin and rabbit polyclonal anti-Cav-1 were purchased from BD PharMingen. Alexa-Fluor 488 and 555-conjugated goat and donkey antimouse or antirabbit IgG were purchased from Life Technologies. Antimouse and antirabbit HRP-conjugated IgG were purchased from Cell Signaling Technology or Kierkegaard and Perry Laboratories (Supporting Information 1). RIPA buffer, protease, and phosphatase inhibitor cocktail, collagenase type I, paraformaldehyde, heparin, and sucrose were purchased from SIGMA Chemical, Co. Mounting media containing DAPI (VectaShield) was obtained from Vector. Stock solutions were prepared in 100% dimethylsulfoxide (DMSO), buffered physiological solution or sterile phosphate-buffered saline (PBS) and diluted daily in sterile PBS or DMEM. The highest final concentration of the solvent was 0.1% (v/v) and did not affect the

experiments. PCR primers were purchased from Integrated DNA Technologies, Inc.

Statistics and scientific rigor

Data were analyzed using GraphPad Prism v9 (GraphPad). Normally distributed data are presented as arithmetic mean \pm standard error of the mean (SEM). Shapiro–Wilk test was used to determine the normality of data and the Brown–Forsythe or *F*-test used to assess equality of variances. Normally distributed data were analyzed using a parametric unpaired Student *t*-test between two groups and parametric Two-way analysis of variance (ANOVA) followed by post hoc analysis (Bonferroni or Tukey Multiple Comparison test) to assess differences between more than two groups with two variables. All tests were performed as two-sided, and $p < 0.05$ was considered statistically significant.

RESULTS

***BMPR2*^{R899X} mutation leads to microvessel muscularization independent of Cav-1 expression**

Silencing or mutation of *BMPR2* promotes cell death and abnormal proliferation of both pulmonary vascular ECs and smooth muscle cells, leading to vascular remodeling and PAH.^{13,23} Similarly, reduced, mutated or absent expression of the anti-inflammatory protein Cav-1 within the lungs contribute to severe vascular remodeling and PAH via elevated eNOS-derived oxidants, depletion of physiologic pulmonary *BMPR2* expression, and disrupted canonical *BMPR2*/phosphorylated-SMAD1/5/8 (P-SMAD1/5/8)-mediated signaling.⁶ Interestingly, these studies revealed that heterozygous mice carrying familial genetic mutation in exon 12 of *BMPR2* (R899X), reduce *BMPR2*-long form (LF) expression and lead to vascular remodeling (Figure 1a,b), consistent with a previous report.²⁴ *BMPR2*^{+R899X} mutant mice also showed low levels of *BMPR2*-short fragment (SF) and reduced expression of P-SMAD1/5/8 relative to controls, with no signs of altered pulmonary Cav-1 expression in normoxia exposed mice (Figure 1a,c). Moreover, although the heterozygous knock-in R899X mutation did not increase the overall microvessel area in 12-month-old mice, it was associated with significant accumulation of pulmonary collagen and expression of α -SMA which were associated with muscularization of pulmonary microvessels (Figure 1b,d).

BMPR2 loss in R899X mutant mice contribute to sex-linked differences in hypoxia-induced PH

Previously, we observed that hypoxia-induced TGF- β secretion promoted PH in mouse models with reduced *BMPR2* expression.⁶ Thus, to further investigate the role of reduced expression of *BMPR2* in heterozygous knock-in *R899X* mutant mice in the onset and progression of PH, WT, and *BMPR2*^{+R899X} mutant mice were exposed for 1 month to hypoxia (10% O₂) or kept under normoxic conditions (21% O₂). In normoxic conditions, RVSP was significantly higher in mutant animals compared to WT mice group (Figure 2a). However, there was no statistically significant difference in RVH between the groups (Figure 2d). Chronic hypoxia exposure elevated RVSP and induced RVH in both WT and *BMPR2*^{+R899X} mutant groups, with a greater effect observed in the mutant mice (Figure 2a,d). Moreover, higher RVSP but not RVH was significantly dependent on sex in animals carrying the heterozygous knock-in *R899X* mutation, as female mice primarily accounted for the elevated RVSP both at normoxia and hypoxia (Figure 2c-f). On the other hand, neither normoxia or hypoxia-mediated increase in RVSP or RVH were sex-linked in the WT group (Figure 2b-e). Lung histological analysis revealed no difference in the overall microvessel thickness and area between sexes in the WT and *BMPR2*^{+R899X} mutant groups (Figure 2g-i), indicating the increase in fully muscularized vessel number or the degree of pulmonary vascular contractility may account for the elevated RVSP observed in the female *BMPR2*^{+R899X} mutant animals. Taken together, these data imply elevated RVSP in mice carrying the human *R899X* mutation is sex-dependent but unlikely dependent on hypoxia-associated microvascular narrowing within the lungs.

Hypoxia-induced RVSP in *BMPR2*^{+R899X} females is associated with eNOS-Cav-1 dichotomy

Prolonged exposure to hypoxia induces structural and functional alterations in the pulmonary vasculature, which strongly varies depending on sex.²⁴ Elevated expression of α -SMA in the pulmonary microcirculation has been extensively used as indicative of microvessel muscularization, and is often associated with increased pulmonary vasoconstriction and vascular resistance, leading to pathological elevation in RVSP that characterizes PAH. The increase in microvascular α -SMA expression occurs in response to different processes, including the expansion and hyperactivation of fibroblasts, myofibroblasts, or muscle-like cells within the vasculature, as observed in response to EndoMT. In line with these observations, our data indicate that

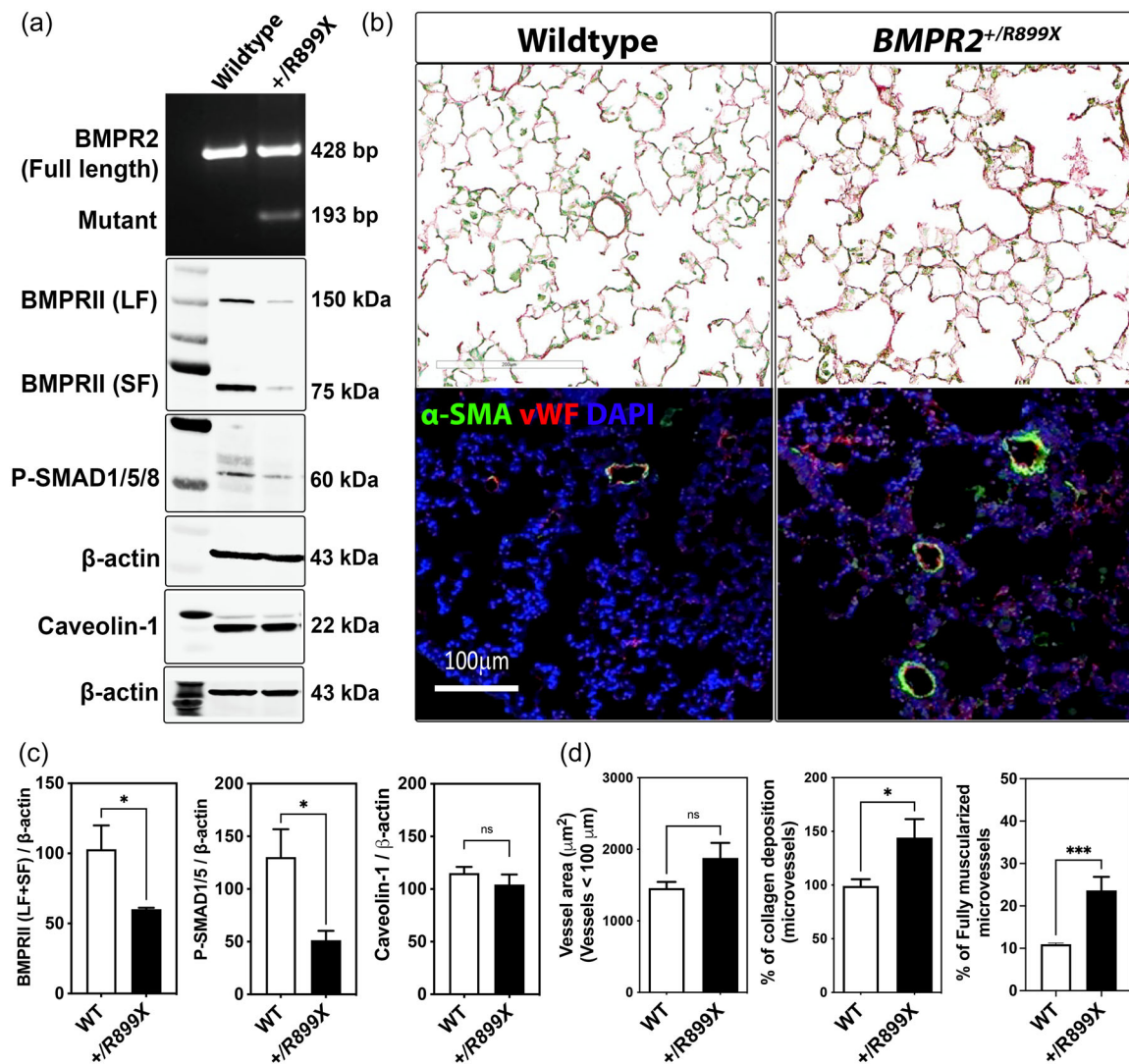


FIGURE 1 Depletion of pulmonary BMPRII-short and long fragments in humanized *BMPR2*^{+/R899X} mutant mice caused vascular remodeling independent of pulmonary caveolin-1 expression under normoxic conditions. Male and female wild type (WT) and *BMPR2*^{+/R899X} mice were genotyped using amplification refractory mutation system PCR (ARMS-PCR) with 428 bp indicating the full-length BMPR2 and 193 bp, amplification of the BMPR2 mutated fragment. Genotyped animals were kept under normoxia for 1 month, and then perfused lung tissue was obtained to evaluate the expression level of BMPRII short and long fragment (SF/LF), phosphorylated-SMAD1/5/8 (P-SMAD1/5/8), β -actin, and caveolin-1 (Cav-1) (a, b) by western blot or fixed for histological analysis of the microvessel area and collagen deposition using Picosirius FAST Red staining (c, d). The percentage of fully muscularized microvessels was quantified using von Willebrand Factor (vWF; Red) and alpha-smooth muscle actin (α -SMA; green) staining (b, d). Normally distributed data were evaluated using the Student *t*-test. **p* < 0.05, ***p* < 0.01, *****p* < 0.001, ns, non significant.

reduced expression of BMPRII protein in the lungs of heterozygous knock-in *R899X* mutant mice increased the number of fully muscularized microvessels, an effect significantly elevated in female animals upon chronic hypoxia exposure (Figure 3a,b). Moreover, our data also showed that chronic hypoxia exposure increased eNOS expression, whereas it reduced the expression of Cav-1, in the lungs of the *BMPR2*^{+/R899X} females but not males (Figure 3c,d). In opposition to the expected increase in eNOS monomers accumulation in unboiled samples, indicative of Cav-1 depletion-dependent eNOS uncoupling, we detected

no difference among the groups (Figure 3e). Since eNOS dysfunction often results in vasoconstrictor endothelin-1 (ET-1) production by ECs, we next assessed ET-1 levels in the lungs of all mutant groups. *BMPR2*^{+/R899X} females exhibited a significant increase in ET-1 levels under normoxic conditions, an effect not sustained under hypoxia exposure (Figure 3f). Altogether, these data suggest *BMPR2*^{+/R899X} mutation has a sex bias, contributing to elevate expression of pulmonary vasoconstrictor ET-1 in female animals at normoxia, and under hypoxia, reducing vasoprotective levels of Cav-1, increasing expression of

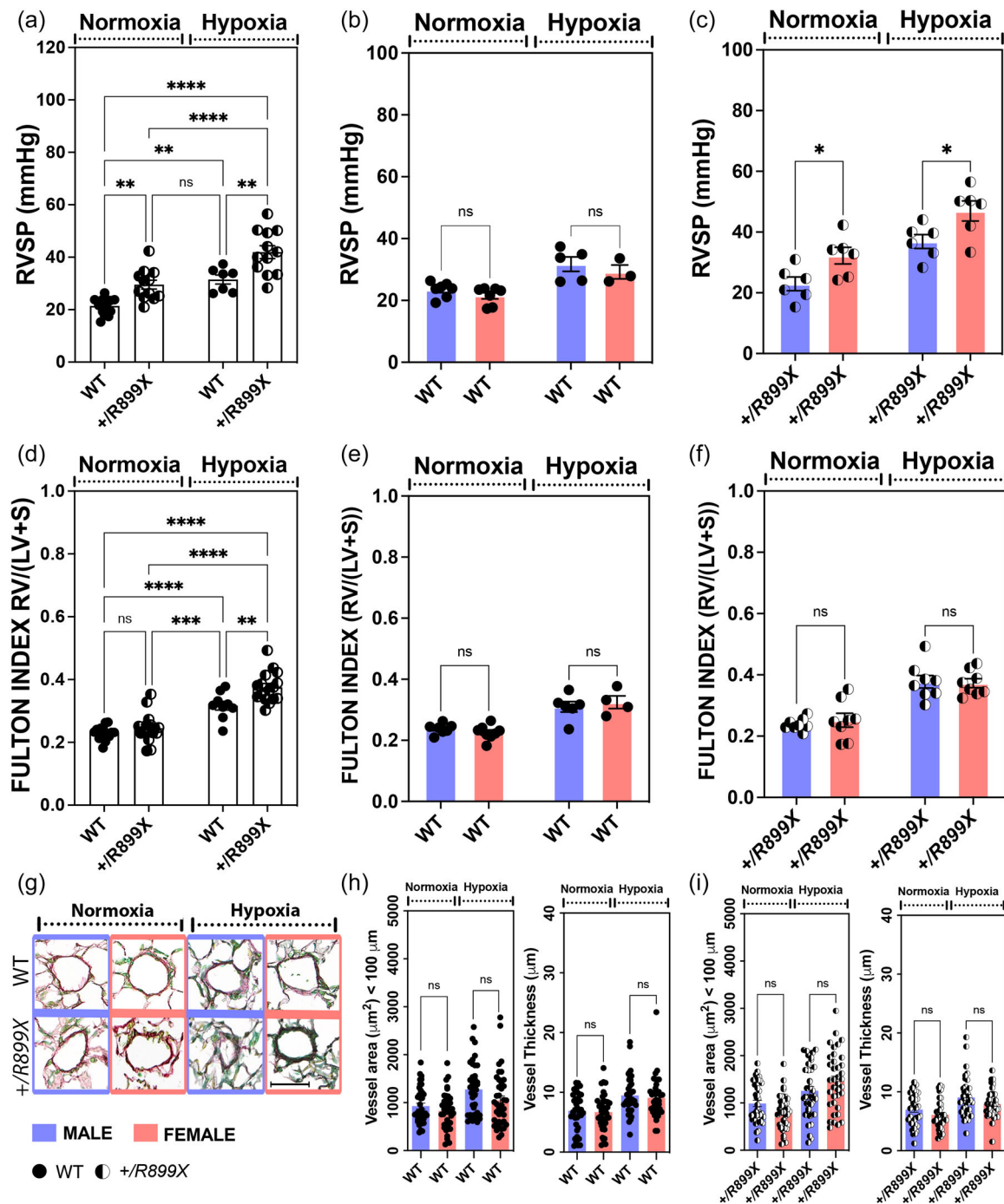


FIGURE 2 *BMPR2*^{+/R899X} mutation predisposes female mice to exhibit elevated pulmonary pressure. Male (blue bars/circles) and female (red bars/circles) wild type (WT: full black circles) and *BMPR2*^{+/R899X} mutant (+/R899X: black/white circles) mice kept under normoxia or hypoxia for 1 month were used to evaluate right ventricular systolic pressure (RVSP; a–c) and right ventricular hypertrophy (RVH; d–f) using the Fulton index (RVH = ratio of the RV by the left ventricle [LV] plus the septum [S]: RV/[LV + S]). Mouse lung sections from both groups were stained using Picrosirius FAST Red, scanned, and the area (μm^2) and thickness (μm) of the pulmonary microvessels with a diameter less than 100 μm (scale bar: 100 μm) were quantified (g–i). Normally distributed data were evaluated using two-way analysis of variance followed by Tukey (a, d) or Bonferroni (b, e, c, f) post hoc test ($n = 7$ –12 animals per group; 6–8 males or females). Data are represented as mean \pm SEM. * $p < 0.05$, ** $p < 0.01$, **** $p < 0.001$, ns, non significant.

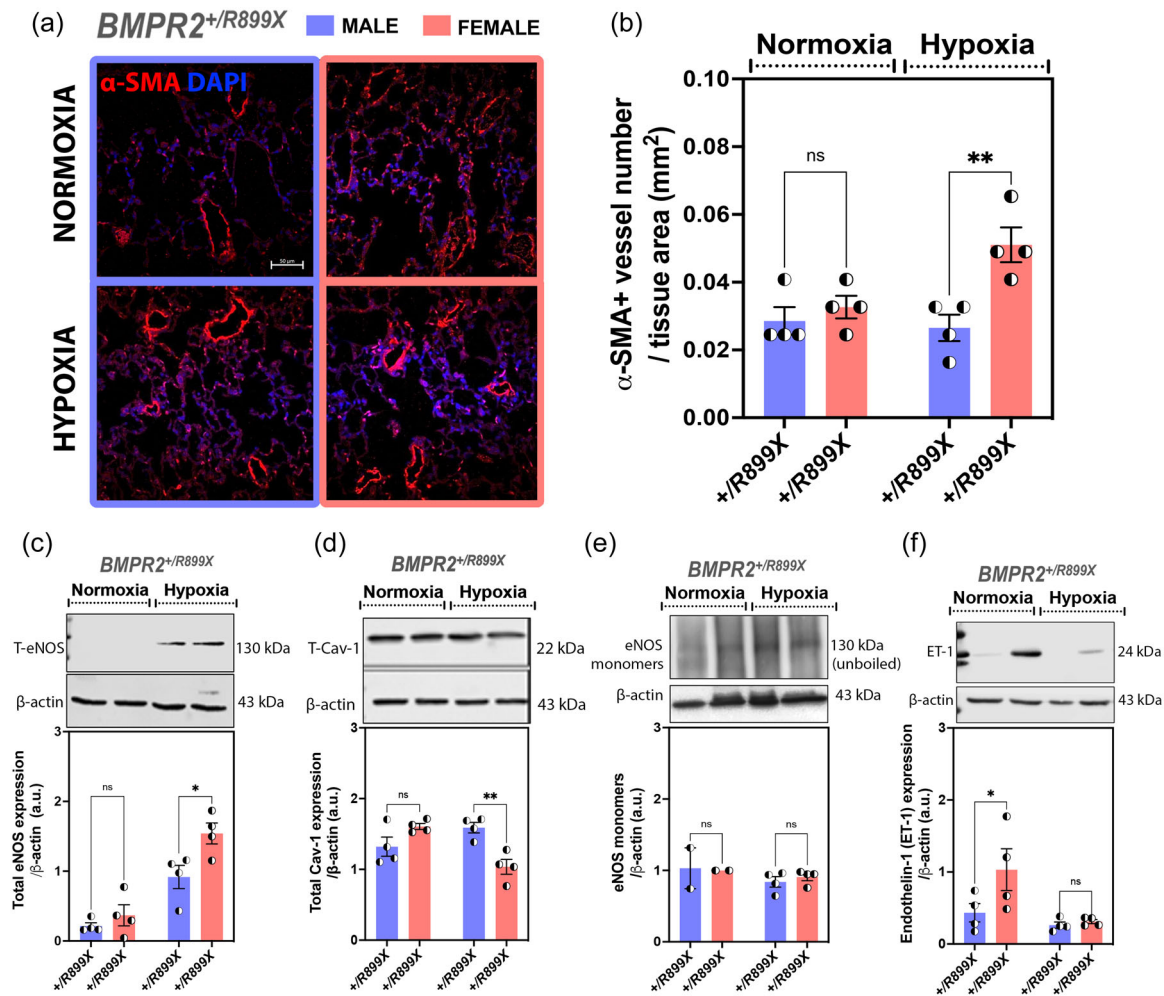


FIGURE 3 Chronic hypoxia exposure increased the number of muscularized microvessels within the lungs of female *BMPR2*^{+/R899X} mutant mice. (a, b) Mouse lung sections from male (light blue bars and circles) and female (light red bars and circles) *BMPR2*^{+/R899X} mice (normoxia and hypoxia) were stained with an antibody against smooth muscle actin (α -SMA; red), and the nuclei stained using DAPI (blue). Then, the number of fully muscularized α -SMA positive pulmonary microvessels with diameters smaller than 100 μ m (scale bar: 50 μ m) were quantified per lung tissue area (mm²; four areas per animal) using confocal microscopy. (c–f) Mouse lung tissue from all groups was used to quantify the expression levels of the total and monomeric endothelial nitric oxide synthase (eNOS), total caveolin-1 (Cav-1), and endothelin-1 (ET-1). β -actin was used as loading control. Normally distributed data were evaluated using two-way analysis of variance followed by Bonferroni post hoc test ($n = 4$ mice per group). * $p < 0.05$, ** $p < 0.01$, ns, non significant.

pulmonary eNOS and the number of muscularized vessels, which seems to align at least in part with the vasoconstrictive/proliferative phases during the course of the disease.

Hypoxia reduced IL-6 but induced TGF- β overexpression in the lungs of female *BMPR2*^{+/R899X} mice

The IL-6/IL-6R-signaling pathway induces Cav-1 depletion and eNOS uncoupling in human pulmonary artery ECs, leading to TGF- β -mediated EndoMT and inflammatory vascular remodeling.⁷ Overexpression of IL-6 per se is also

known to increase TGF- β -mediated signaling by reducing TGF-RI association with Cav-1,²⁵ thereby promoting vascular remodeling and PH in mice.²⁶ Thus, to evaluate whether hypoxia-induced PH in *BMPR2*^{+/R899X} female mice is associated with an inflammatory component, especially related to pro-fibrotic signaling via IL-6 and TGF- β , we quantified these inflammatory signals in the lungs of WT and mutant animals at normoxia and following chronic hypoxia exposure. Although hypoxia significantly increased IL-6 levels in the lungs of WT animals, no significant differences were observed between sexes (Figure 4a). Interestingly, the lungs of female *BMPR2*^{+/R899X} mutant mice showed lower levels of IL-6 compared to male animals under normoxia or after chronic hypoxia exposure,

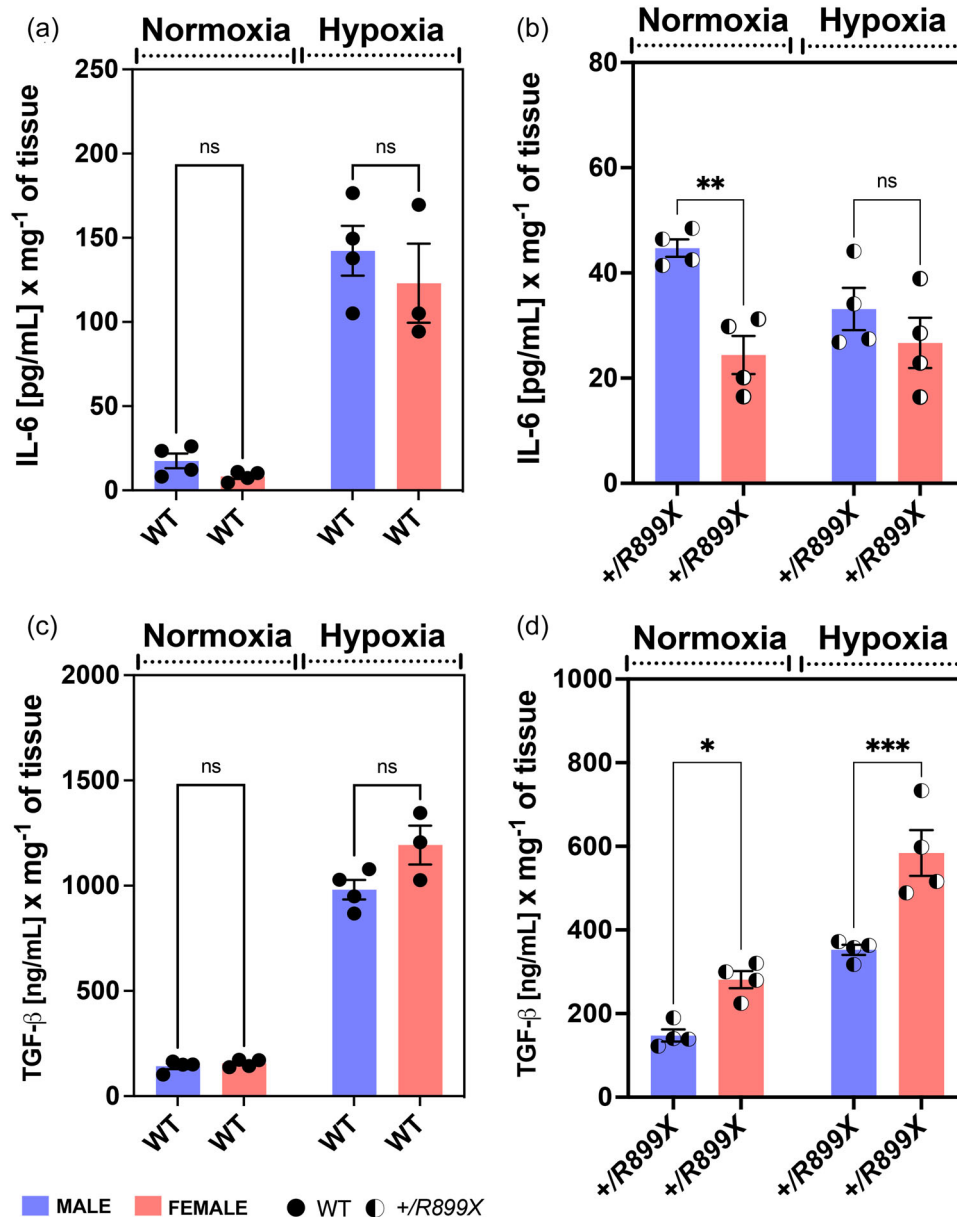


FIGURE 4 Chronic hypoxia exposure reduced interleukin (IL)-6 and upregulated TGF- β level in the lungs of $BMPR2^{+/R899X}$ females. Mouse lung tissue from male (light blue bars) and female (light red bars) $BMPR2^{+/R899X}$ mice at normoxia and hypoxia were used to quantify: IL-6 level per milligram (mg) of lung tissue in WT (a) and $BMPR2^{+/R899X}$ mutants (b) or TGF- β per mg of lung tissue in WT (c) and $BMPR2^{+/R899X}$ mutants (d). Inset: dark and white circles represent individual $BMPR2^{+/R899X}$ mutant mice ($n = 4$ animals per group). Normally distributed data were evaluated using two-way analysis of variance followed by Bonferroni post hoc test. * $p < 0.05$, ** $p < 0.01$, *** $p < 0.001$, ns, non significant.

indicating IL-6-mediated signaling may not account for sex differences observed in $BMPR2^{+/R899X}$ mutant mice (Figure 4b). Similarly, pulmonary TGF- β levels increased upon hypoxia exposure in WT male and female animals (Figure 4c). Measurements of pulmonary TGF- β levels in $BMPR2^{+/R899X}$ mutant mice revealed that chronic hypoxia enhances TGF- β secretion in both sexes, however, in opposition to that observed in the WT group, females displayed higher levels even in normoxic conditions (Figure 4d). These results suggest enhanced TGF- β -mediated pro-fibrotic signaling may contribute to increased

incidence of microvascular muscularization in female $BMPR2^{+/R899X}$ mutant mice.

$BMPR2^{+/R899X}$ mutation expands TGF- β -producing myfibroblasts within the lung microvasculature

Increased α -SMA expression and collagen production, which are characteristics of fibroblasts and myfibroblasts derived from several cellular processes, including

EndoMT, contribute to vascular remodeling. In fact, studies herein revealed that besides elevated collagen deposition and an increase in the number of α -SMA+ microvessels, as shown in Figures 1b, 3a,b, accumulation of fibroblast-specific protein-1 (FSP-1) was also observed in pulmonary precapillary resistance vessels of *BMPR2*^{+/*R899X*} mutant animals as opposed to WT controls (Figure 5a,b). Moreover, when isolated, the proliferation rate of *BMPR2*^{+/*R899X*}-derived pulmonary fibroblasts²² (characterized by expression of HSP47²⁷ and PHD4²⁸) was twofold higher than WT mouse-derived cells (Figure 5c-f), which may also contribute to the increased number of fully muscularized microvessels observed in *BMPR2*^{+/*R899X*} mutants. Finally, *BMPR2*^{+/*R899X*}-derived pulmonary fibroblasts expressed higher levels of collagen and matrix metalloproteinase 9 (MMP9) and secreted more TGF- β than WT fibroblasts (Figure 5g,h), indicating *BMPR2*^{+/*R899X*}-induced loss-of-function increases the percentage of activated myofibroblasts leading to microvascular muscularization, elevated pulmonary pressure, and PAH.

DISCUSSION

Substantial evidence indicates that progression of pulmonary vascular remodeling during PAH occurs as a dual-phase process. First, there is an apoptotic phase in which cells within the pulmonary vascular wall are damaged, and second, in an abnormal proliferative phase, the vascular cells that were able to survive the apoptotic stimuli undergo epigenetic reprogramming, proliferate and alter the structure of the pulmonary vasculature, leading to the formation of chronic inflammatory vascular lesions.^{2,3,6,29,30} Identification of the molecular mechanisms that trigger pulmonary vascular injury and promote vascular remodeling remains an important goal to advance the field and shed light on new therapeutic approaches and molecular targets.³⁰ Accordingly, several EC-associated biological processes, including apoptosis-resistant cell growth and EndoMT, have been implicated in the onset and severity of cardiopulmonary diseases, including PAH.²⁹⁻³¹ Most interestingly, all of these processes seem to convey the idea that chronically-injured pulmonary endothelium attempts but is unable to heal itself, and thus, affected lung vessels become remodeled and occluded over time leading to PAH.

In support of these well-accepted findings, despite the fact that initiating events that promote alterations in the healthy endothelium remain not fully clear, reduced expression and mutations of the antiproliferative and

anti-inflammatory proteins Cav-1 and BMPR2 as a result of lung vascular injury, have been shown to significantly contribute for the progression of PAH.^{6,32-35} Moreover, loss of pulmonary endothelial Cav-1 expression plays a key role in impaired BMPR2-mediated signaling and increased TGF- β production by macrophages, which in turn promotes the expansion of abnormal Cav1-depleted ECs.⁶ Of note, both BMPR2-LF and SF have been found associated with Cav-1,^{36,37} while endocytosis of BMPR2-SF appears to be uniquely dependent on caveolae.³⁸ Although poorly described, increased expression of the BMPR2-SF splice variant on the cell surface correlates with increased P-SMAD1/5/8 signaling, suggesting BMPR2-SF depletion may be a major player in impaired SMAD1/5/8 phosphorylation and signaling. Here, we observed that *BMPR2*^{+/*R899X*} mutant mice showed a reduction of both fragments in their lungs, and as consequence, lower phosphorylation of pulmonary SMAD1/5/8. Despite strong evidence in support of the role of reduced BMPR2 expression and signaling in the onset and progression of PAH, as well as ongoing efforts to target BMPR2-associated signaling to reduce PAH morbidity, how lung ECs with reduced BMPR2 expression contribute to pulmonary vascular remodeling remain under extensive investigation.

Chronic hypoxia induces structural and functional alterations in the pulmonary vasculature, which strongly varies depending on species, developmental stage, and sex.²⁴ In fact, the studies presented here indicate that hypoxia-induced PH in *BMPR2*^{+/*R899X*} mutant mice is sex-linked, since it recapitulates at the least in part, the clinical pattern of increased incidence of PAH in females. It is well-known that hypoxia induces vasoconstriction, EndoMT, and remodeling of the pulmonary vasculature which varies in magnitude depending on sex.²⁴ Recent data by Frump et al.¹⁸ revealed that BMPR2 expression is in fact required for 17 β -estradiol (E2) and apelin-mediated cardioprotective effects on the RV of mice and rats, which addresses a potentially important mechanism by which females have a better PAH prognosis than their male counterparts despite higher disease incidence in females. In line with these observations, Umar and colleagues also showed that estrogen has been shown to reverse severe PH in rats via cardiopulmonary neoangiogenesis and suppression of inflammation, fibrosis, and RV hypertrophy.³⁹ Indeed, E2 directly affects vascular ECs, at least in part, by stimulating the expression and function of the eNOS.⁴⁰⁻⁴² Here, data indicate that although the 1-month hypoxia exposure did not significantly change the degree of RVH in male or female *BMPR2*^{+/*R899X*} mutant as compared to normoxia exposed mice, it increased RVSP in females despite higher level of eNOS expression. Although these

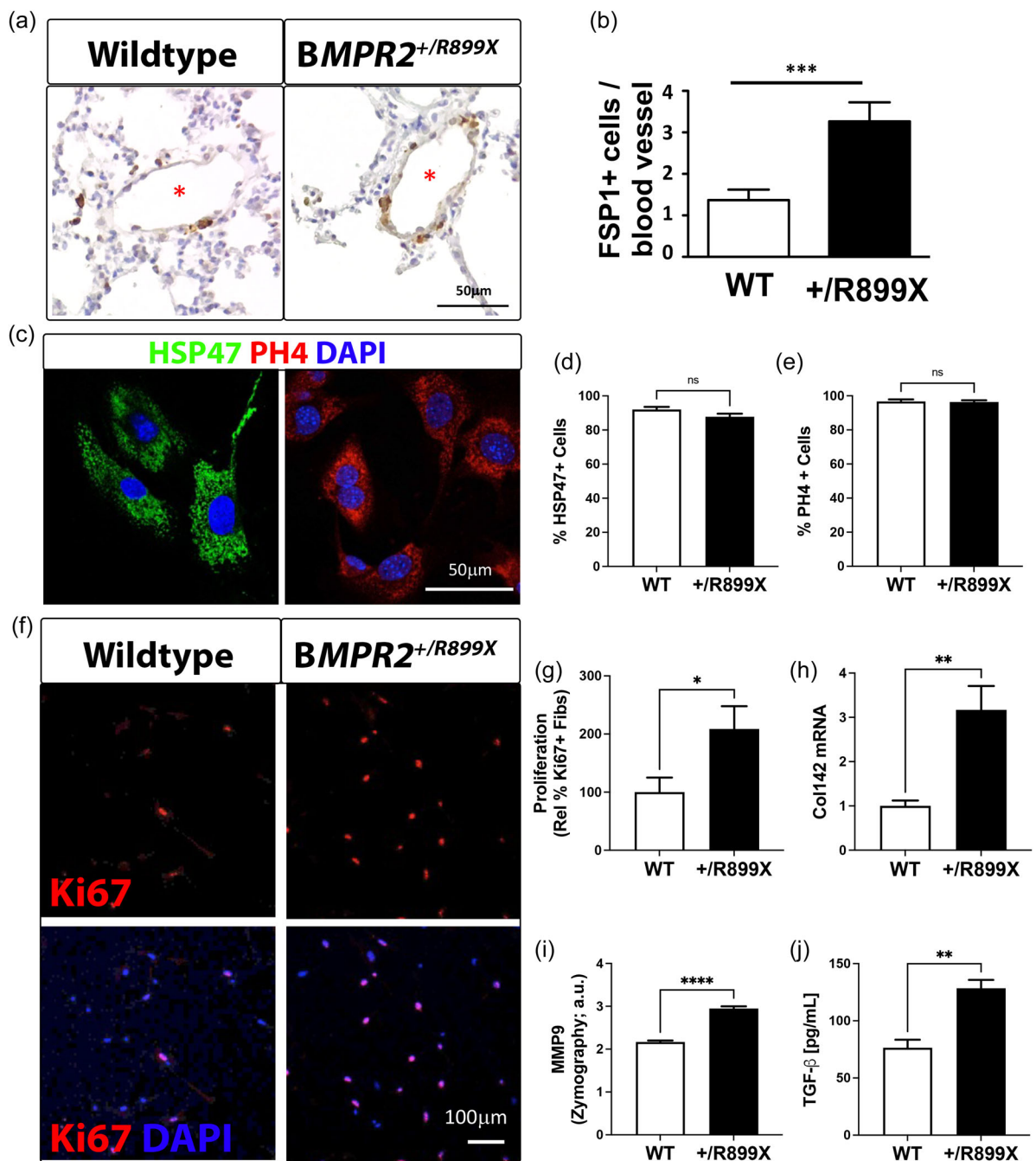


FIGURE 5 *BMPR2^{+/R899X}* mutation leads to the accumulation of hyperproliferative myofibroblasts in the pulmonary circulation. (a, b) Mouse lung sections from male and female wild type (WT) and *BMPR2^{+/R899X}* mutant mice were stained using fibroblast-specific protein-1 (FSP-1) (brown) and the number of fibroblasts per blood vessel was quantified. Blood vessel lumen is indicated with a red asterisk. Fibroblasts were isolated from male and female wild type (WT) and *BMPR2^{+/R899X}* mutant mice and stained using antibodies against HSP47 (green) or PH4 (red), and DAPI (blue), and the percentage of HSP47+ and PH4+ fibroblasts quantified. (c–e) Isolated pulmonary fibroblasts from WT and *BMPR2^{+/R899X}* mice were used to quantify the expression of Ki67 (red), indicative of proliferation (f, g), expression of Col1A2 (h), matrix metalloproteinase 9 (MMP9; i) activity, and secretion of TGF-β (j). Normally distributed data were evaluated using student *t*-test. **p* < 0.05, ***p* < 0.01, ****p* < 0.001, ns, non significant.

data suggest oxidant-associated eNOS monomers do not accumulate in the lungs of *BMPR2^{+/R899X}* female mice, elevated ET-1 levels at normoxia may contribute to the spontaneous increase in RVSP, followed by a hyperproliferative phase. Previous studies have reported that

elevated level of ET-1 and eNOS-associated oxidative stress have potent vasoconstrictor effects during the course of PH.^{43–46} Moreover, inflammatory cytokines such as IL-6 and TGF-β are known to promote eNOS dysfunction and oxidant generation leading to EndoMT

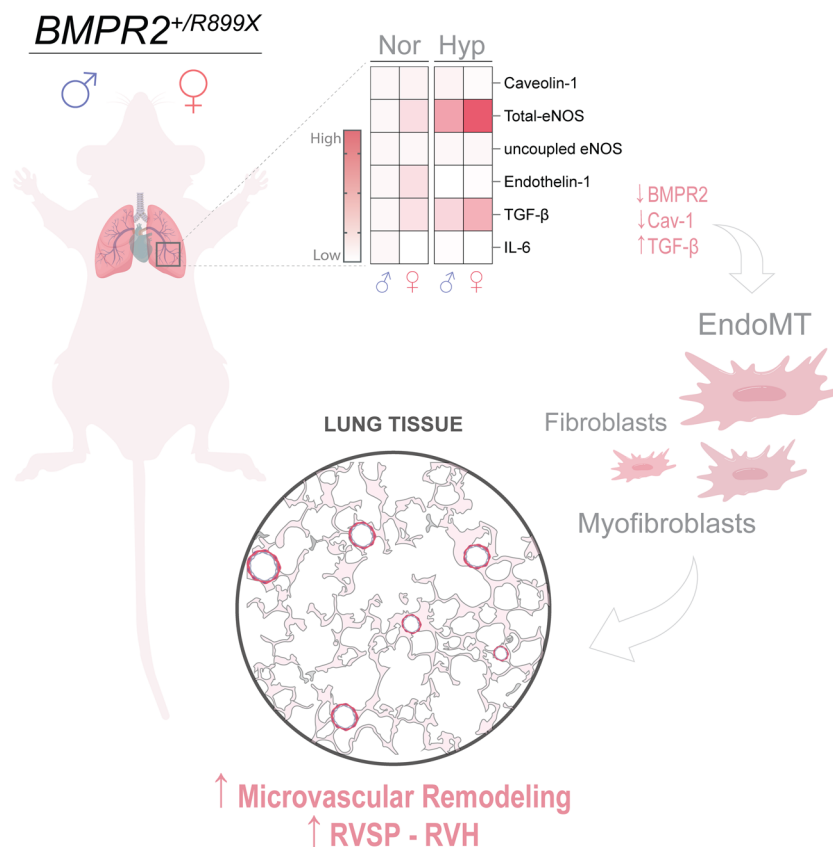


FIGURE 6 Role of hypoxia-induced PH on sex-linked differences in humanized *BMPR2*^{+/R899X} mutant mice. Upon chronic hypoxia exposure, male humanized *BMPR2*^{+/R899X} mutant mice (left side; light blue symbol) showed loss of Bone Morphogenetic Protein Receptor II (BMPRII) expression, unchanged expression of the protein Caveolin-1 and mild elevation in the expression levels of the endothelial nitric oxide synthase (eNOS) and transforming growth factor- β (TGF- β) in the lungs, leading to microvascular muscularization and elevated right ventricular systolic pressure (RVSP), an effect highly exacerbated in female *BMPR2*^{+/R899X} humanized animals (right side; light red), whom also showed reduced expression of the vasoprotective protein caveolin-1 in their lungs. On the other hand, right ventricular hypertrophy (RVH) was equally increased between *BMPR2*^{+/R899X} sexes upon chronic hypoxia exposure. At normoxia, pulmonary Endothelin-1 levels is elevated in female mutants compared to males, but unaltered upon hypoxia. Inset: Red/green circles represents muscularized microvessels within the lung tissue (in gray). Pink cells represent fibroblasts and myofibroblasts derived or not from endothelial-to-mesenchymal transition (EndoMT).

and PAH.^{7,26} Thus, we evaluated whether hypoxia-induced PH in *BMPR2*^{+/R899X} mice is associated with a significant inflammatory component. Results indicate that hypoxia-induced TGF- β upregulation varies with sex in *BMPR2*^{+/R899X} mutant mice. Moreover, our studies also indicated that a spontaneous increase in pulmonary TGF- β level occurs in *BMPR2*^{+/R899X} female mice. Besides the strong role of TGF- β in PAH, this fibrosis-associated cytokine has also been implicated as a potent stimulus for ET-1 via ALK-5/SMAD2/3 activation in chronic thromboembolic PH.⁴⁶ Indeed, TGF- β -mediated ALK-5/SMAD2/3 exacerbates PH in mice lacking EC-Cav-1 expression and contributes to EndoMT.^{6,7} Also, IL-6 was associated with poor survival in PAH patients,⁴⁷ and was elevated in human PAH male patients as compared to females.⁴⁸ Thus, reduced IL-6 in the lungs of female *BMPR2*^{+/R899X} animals might contribute to

improved disease prognosis. Of note, although *BMPR2*^{+/R899X} mutant animals exposed to hypoxia appear to have reduced IL-6 and TGF- β lung tissue level when compared to WT animals, measurements were performed in separate experiments, and thus sex comparisons herein are only made within the same genotype. Altogether, these findings indicate that *BMPR2*^{+/R899X} mutation in female mice substantially contribute to increase profibrotic TGF- β and vasoactive ET-1 levels which may contribute to lung EC activation and de-differentiation into hyperproliferative myofibroblast-like phenotype that contribute to microvascular muscularization, remodeling, and PAH (Figure 6).

EndoMT, myofibroblasts, or activated fibroblasts - despite the terminology, it is unmistakably evident that all those processes culminate in the generation of a proliferative collagen-producing phenotype with high

expression of muscle markers such as α -SMA, which in turn contributes to increased vascular tone in the normally low resistance arteries within the lungs.^{47,48} The specific molecular mechanisms that give rise to these cell phenotypes require further investigation. Nonetheless, a substantial amount of evidence implicates elevated TGF- β as the major determinant of the transformation of vascular cells into abnormal apoptosis-resistant hyperproliferative cell types.^{6,49,50} Furthermore, it is unclear how defective BMPR2 and hyperactivated TGF- β -mediated signaling first emerges, or how sex-associated differences contribute to elevated RVSP in females. Here, our data indicate that the density of proliferative fibroblast-like cells is spontaneously elevated within the vascular wall of small pulmonary resistance vessels in *BMPR2^{+ / R899X}* mutant mice. Moreover, we identified that this cell population is hyperactivated and contributes to elevated collagen deposition in the lung vasculature of *BMPR2^{+ / R899X}* mutants, as well as the elevated number of pulmonary α -SMA+ microvessels in the hypoxia-exposed *BMPR2^{+ / R899X}* female animals. Since dysfunctional ECs also produce increased levels of pro-proliferative factors such as ET-1,^{51,52} perhaps it may be an alternative mechanism for stimulating the proliferation of fibroblast-like cells and increase RVSP in females. Finally, we observed that *BMPR2^{+ / R899X}*-derived fibroblast-like cells produced high levels of TGF- β and expressed higher levels of activated MMP9, an enzyme previously reported to be important in the pathogenesis of PAH. This reinforces the significant role of *BMPR2^{+ / R899X}* mutation and loss of functional BMPR2 expression within the lung vasculature in the development of PAH, especially in terms of the sexual dimorphism-associated with the disease.

AUTHOR CONTRIBUTIONS

Suellen D. Oliveira, Richard D. Minshall, and Glenn Marshboom conceived and planned the experiments. Suellen D. Oliveira, Ejehi O. Erewele, Maricela Castellon, Omar Loya, Glenn Marshboom, Andrew Schwartz, Kayla Yerlioglu, Christopher Callahan, and Jiwang Chen contributed to sample preparation. Suellen D. Oliveira, Glenn Marshboom, Ejehi O. Erewele, Omar Loya, and Jiwang Chen contributed to graph preparation, statistical analysis, and interpretation of results. Suellen D. Oliveira, Ejehi O. Erewele, and Omar Loya carried out the histological analysis, western blots, and ELISA measurements. Glenn Marshboom conceived, carried out, and analyzed the fibroblast-related experiments. Maricela Castellon and Kayla Yerlioglu performed strain genotyping, sex randomization, and hypoxia exposure. Jiwang Chen collected data of the right ventricle systolic pressure and right ventricular hypertrophy.

ACKNOWLEDGMENTS

We thank Dr. Nicholas W. Morrell (Professor of Medicine; University of Cambridge - United Kingdom) for providing the *BMPR2^{+ / R899X}* mutant mice and for critically reading the manuscript. We also thank the University of Illinois at Chicago Research Resources Cores facilities for assistance with Histology and Imaging and the Graphic Designer Pedro C. H. Simões for support in generating Figure 6. This work was supported in part by a Catalyst Award from the American Lung Association and a K01 award from the National Institutes of Health/National Heart, Lung, and Blood Institute (ALA 697907; NIH HL159037, respectively—Oliveira, SDS), National Institutes of Health (NIH HL142636—Minshall, RD), a scholarship from the College of Medicine Urban Health Research Program (COM-UHP—Erewele, EO), and a scholarship from UIC Latin@s Gaining Access to Networks for Advancement in Science (L@s GANAS - Omar Loya).

CONFLICT OF INTEREST

The authors declare no conflict of interest.

ETHICS STATEMENT

All animal experiments in this study were performed as approved by the University of Illinois at Chicago Institutional Animal Care and Use Committee.

ORCID

Suellen D. Oliveira  <https://orcid.org/0000-0002-7654-1909>

REFERENCES

1. Evans JDW, Girerd B, Montani D, Wang XJ, Galie N, Austin ED, Elliott G, Asano K, Grünig E, Yan Y, Jing ZC, Manes A, Palazzini M, Wheeler LA, Nakayama I, Satoh T, Eichstaedt C, Hinderhofer K, Wolf M, Rosenzweig EB, Chung WK, Soubrier F, Simonneau G, Sitbon O, Gräf S, Kaptoge S, Di Angelantonio E, Humbert M, Morrell NW. *BMPR2* mutations and survival in pulmonary arterial hypertension: an individual participant data meta-analysis. *Lancet Respirat Med*. 2016;4(2):129–37.
2. Sakao S, Tatsumi K, Voelkel NF. Endothelial cells and pulmonary arterial hypertension: apoptosis, proliferation, interaction and transdifferentiation. *Respir Res*. 2009;10(1):95.
3. Voelkel NF, Gomez-Arroyo J, Abbate A, Bogaard HJ, Nicolls MR. Pathobiology of pulmonary arterial hypertension and right ventricular failure. *Eur Respir J*. 2012;40(6):1555–65.
4. Simonneau G, Montani D, Celermajer DS, Denton CP, Gatzoulis MA, Krowka M, Williams PG, Souza R. Haemodynamic definitions and updated clinical classification of pulmonary hypertension. *Eur Respir J*. 2019;53(1):1801913.
5. Evans CE, Cober ND, Dai Z, Stewart DJ, Zhao YY. Endothelial cells in the pathogenesis of pulmonary arterial hypertension. *Eur Respir J*. 2021;58(3):2003957.

6. Oliveira SDS, Chen J, Castellon M, Mao M, Raj JU, Comhair S, Erzurum S, Silva CLM, Machado RF, Bonini MG, Minshall RD. Injury-Induced shedding of extracellular vesicles depletes endothelial cells of Cav-1 (Caveolin-1) and enables TGF- β (transforming growth factor- β)-dependent pulmonary arterial hypertension. *Arterioscler Thromb Vasc Biol.* 2019;39(6):1191–202.
7. Oliveira SDS, Castellon M, Chen J, Bonini MG, Gu X, Elliott MH, Machado RF, Minshall RD. Inflammation-induced caveolin-1 and BMPRII depletion promotes endothelial dysfunction and TGF- β -driven pulmonary vascular remodeling. *Am J Physiol Lung Cell Mol Physiol.* 2017;312(5):L760–71.
8. Piera-Velazquez S, Li Z, Jimenez SA. Role of endothelial-mesenchymal transition (EndoMT) in the pathogenesis of fibrotic disorders. *Am J Pathol.* 2011;179(3):1074–80.
9. Gangopahyay A, Oran M, Bauer EM, Wertz JW, Comhair SA, Erzurum SC, Bauer PM. Bone morphogenetic protein receptor II is a novel mediator of endothelial nitric-oxide synthase activation. *J Biol Chem.* 2011;286(38):33134–40.
10. Frump A, Prewitt A, Caestecker MP. BMPR2 mutations and endothelial dysfunction in pulmonary arterial hypertension (2017 grover conference series). *Pulm Circ.* 2018;8:1–12.
11. Machado RD, Pauciulo MW, Thomson JR, Lane KB, Morgan NV, Wheeler L, Phillips III JA, Newman J, Williams D, Galiè N, Manes A, McNeil K, Yacoub M, Mikhail G, Rogers P, Corris P, Humbert M, Donnai D, Martensson G, Tranebjaerg L, Loyd JE, Trembath RC, Nichols WC. BMPR2 haploinsufficiency as the inherited molecular mechanism for primary pulmonary hypertension. *Am J Hum Genet.* 2001;68(1):92–102.
12. Deng Z, Morse JH, Slager SL, Cuervo N, Moore KJ, Venetos G, Kalachikov S, Cayanis E, Fischer SG, Barst RJ, Hodge SE, Knowles JA. Familial primary pulmonary hypertension (gene PPH1) is caused by mutations in the bone morphogenetic protein receptor-II gene. *Am J Hum Genet.* 2000;67(3):737–44.
13. Long L, Ormiston ML, Yang X, Southwood M, Gräf S, Machado RD, Mueller M, Kinzel B, Yung LM, Wilkinson JM, Moore SD, Drake KM, Aldred MA, Yu PB, Upton PD, Morrell NW. Selective enhancement of endothelial BMPR-II with BMP9 reverses pulmonary arterial hypertension. *Nature Med.* 2015;21(7):777–85.
14. Ge X, Zhu T, Zhang X, Liu Y, Wang Y, Zhang W. Gender differences in pulmonary arterial hypertension patients with BMPR2 mutation: a meta-analysis. *Respir Res.* 2020;21(1):44.
15. Austin ED, Hamid R, Hemnes AR, Loyd JE, Blackwell T, Yu C, Phillips III JA, Gaddipati R, Gladson S, Gu E, West J, Lane KB. BMPR2 expression is suppressed by signaling through the estrogen receptor. *Biol Sex Differ.* 2012;3(1):6.
16. Liu D, Wu W-H, Mao Y-M, Yuan P, Zhang R, Ju FL, Jing ZC. BMPR2 mutations influence phenotype more obviously in male patients with pulmonary arterial hypertension. *Circ Cardiovasc Genet.* 2012;5(5):511–8.
17. Cheron C, McBride SA, Antigny F, Girerd B, Chouchana M, Chaumais MC, Jaïs X, Bertoletti L, Sitbon O, Weatherald J, Humbert M, Montani D. Sex and gender in pulmonary arterial hypertension. *Eur Respir Rev.* 2021;30(162):200330.
18. Frump AL, Albrecht M, Yakubov B, Breuils-Bonnet S, Nadeau V, Tremblay E, Potus F, Omura J, Cook T, Fisher A, Rodriguez B, Brown RD, Stenmark KR, Rubinstein CD, Krentz K, Tabima DM, Li R, Sun X, Chesler NC, Provencher S, Bonnet S, Lahm T. 17 β -estradiol and estrogen receptor α protect right ventricular function in pulmonary hypertension via BMPR2 and apelin. *J Clin Invest.* 2021;131(6):e129433. <https://doi.org/10.1172/JCI129433>
19. Little S. Amplification-refractory mutation system (ARMS) analysis of point mutations. *Curr Prot Hum Genet.* 1995;7(1). <https://doi.org/10.1002/0471142905.hg0908s07>
20. Chen J, Sysol JR, Singla S, Zhao S, Yamamura A, Valdez-Jasso D, Abbasi T, Shioura KM, Sahni S, Reddy V, Sridhar A, Gao H, Torres J, Camp SM, Tang H, Ye SQ, Comhair S, Dweik R, Hassoun P, Yuan JXJ, Garcia JGN, Machado RF. Nicotinamide phosphoribosyltransferase promotes pulmonary vascular remodeling and is a therapeutic target in pulmonary arterial hypertension. *Circulation.* 2017;135(16):1532–46.
21. Oliveira SDS, Quintas LEM, Amaral LS, Noël F, Farsky SH, Silva CLM. Increased endothelial cell-leukocyte interaction in murine schistosomiasis: possible priming of endothelial cells by the disease. *PLoS One.* 2011;6(8):e23547.
22. Marsboom G, Chen Z, Yuan Y, Zhang Y, Tirupathi C, Loyd JE, Austin ED, Machado RF, Minshall RD, Rehman J, Malik AB. Aberrant caveolin-1-mediated Smad signaling and proliferation identified by analysis of adenine 474 deletion mutation (c.474delA) in patient fibroblasts: a new perspective on the mechanism of pulmonary hypertension. *Mol Biol Cell.* 2017;28(9):1177–85.
23. Yu PB, Beppu H, Kawai N, Li E, Bloch KD. Bone morphogenetic protein (BMP) type II receptor deletion reveals BMP ligand-specific gain of signaling in pulmonary artery smooth muscle cells. *J Biol Chem.* 2005;280(26):24443–50.
24. Stenmark KR, Fagan KA, Frid MG. Hypoxia-induced pulmonary vascular remodeling. *Circ Res.* 2006;99(7):675–91.
25. Zhang XL, Topley N, Ito T, Phillips A. Interleukin-6 regulation of transforming growth factor (TGF)- β receptor compartmentalization and turnover enhances TGF- β 1 signaling. *J Biol Chem.* 2005;280(13):12239–45.
26. Steiner MK, Syrkina OL, Kolliputi N, Mark EJ, Hales CA, Waxman AB. Interleukin-6 overexpression induces pulmonary hypertension. *Circ Res.* 2009;104(2):236–44.
27. Ito S, Nagata K. Biology of Hsp47 (Serpin H1), a collagen-specific molecular chaperone. *Semin Cell Dev Biol.* 2017;62:142–51.
28. Gorres KL, Raines RT. Prolyl 4-hydroxylase. *Crit Rev Biochem Mol Biol.* 2010;45(2):106–24.
29. Tuder RM, Groves B, Badesch DB, Voelkel NF. Exuberant endothelial cell growth and elements of inflammation are present in plexiform lesions of pulmonary hypertension. *Am J Pathol.* 1994;144(2):275–85.
30. Cool CD, Kuebler WM, Bogaard HJ, Spiekerkoetter E, Nicolls MR, Voelkel NF. The hallmarks of severe pulmonary arterial hypertension: the cancer hypothesis - ten years later. *Am J Physiol Lung Cell Mol Physiol.* 2020;318:L1115–30. <https://doi.org/10.1152/ajplung.00476.2019>
31. Sakao S, Taraseviciene-Stewart L, Lee JD, Wood K, Cool CD, Voelkel NF. Initial apoptosis is followed by increased proliferation of apoptosis-resistant endothelial cells. *FASEB J.* 2005;19(9):1178–80.
32. Oliveira SDS, Minshall RD. Caveolin and endothelial NO signaling. *Curr. Top. Membr.* 2018; 82:257–79.

33. Hopper RK, Moonen J-RAJ, Diebold I, Cao A, Rhodes CJ, Tojais NF, Hennigs JK, Gu M, Wang L, Rabinovitch M. In pulmonary arterial hypertension, reduced BMPR2 promotes endothelial-to-mesenchymal transition via HMGA1 and its target slug. *Circulation*. 2016;133(18):1783–94.
34. Hurst LA, Dunmore BJ, Long L, Crosby A, Al-Lamki R, Deighton J, Southwood M, Yang X, Nikolic MZ, Herrera B, Inman GJ, Bradley JR, Rana AA, Upton PD, Morrell NW. TNF α drives pulmonary arterial hypertension by suppressing the BMP type-II receptor and altering NOTCH signalling. *Nat Commun*. 2017;8:14079.
35. Hartung A, Bitton-Worms K, Rechtman MM, Wenzel V, Boergermann JH, Hassel S, Henis YI, Knaus P. Different routes of bone morphogenetic protein (BMP) receptor endocytosis influence BMP signaling. *Mol Cell Biol*. 2006;26(20):7791–805.
36. Amsalem AR, Marom B, Shapira KE, Hirschhorn T, Preisler L, Paarmann P, Knaus P, Henis YI, Ehrlich M. Differential regulation of translation and endocytosis of alternatively spliced forms of the type II bone morphogenetic protein (BMP) receptor. *Mol Biol Cell*. 2016;27(4):716–30.
37. Nohe A, Keating E, Underhill TM, Knaus P, Petersen NO. Dynamics and interaction of caveolin-1 isoforms with BMP-receptors. *J Cell Sci*. 2005;118(3):643–50.
38. Umar S, Iorga A, Matori H, Nadadur RD, Li J, Maltese F, van der Laarse A, Eghbali M. Estrogen rescues preexisting severe pulmonary hypertension in rats. *Am J Respir Crit Care Med*. 2011;184(6):715–23.
39. Hisamoto K, Ohmichi M, Kurachi H, Hayakawa J, Kanda Y, Nishio Y, Adachi K, Tasaka K, Miyoshi E, Fujiwara N, Taniguchi N, Murata Y. Estrogen induces the akt-dependent activation of endothelial nitric-oxide synthase in vascular endothelial cells. *J Biol Chem*. 2001;276(5):3459–67.
40. Yang S, Bae L, Zhang L. Estrogen increases eNOS and NOX release in human coronary artery endothelium. *J Cardiovasc Pharmacol*. 2000;36(2):242–7.
41. Chen Z, Yuhanna IS, Galcheva-Gargova Z, Karas RH, Mendelsohn ME, Shaul PW. Estrogen receptor α mediates the nongenomic activation of endothelial nitric oxide synthase by estrogen. *J Clin Invest*. 1999;103(3):401–6.
42. Suvorava T, Nagy N, Pick S, Lieven O, R  ther U, Dao VT, Fischer JW, Weber M, Kojda G. Impact of eNOS-dependent oxidative stress on endothelial function and neointima formation. *Antioxid Redox Signaling*. 2015;23(9):711–23.
43. Belik J, Jankov RP, Pan J, Tanswell AK. Peroxynitrite inhibits relaxation and induces pulmonary artery muscle contraction in the newborn rat. *Free Radic Biol Med*. 2004;37(9):1384–92.
44. Yan S, Resta TC, Jernigan NL. Vasoconstrictor mechanisms in chronic hypoxia-induced pulmonary hypertension: role of oxidant signaling. *Antioxidants*. 2020;9(10):999.
45. Zhao YY, Zhao YD, Mirza MK, Huang JH, Potula HHSK, Vogel SM, Brovkovych V, Yuan JXJ, Wharton J, Malik AB. Persistent eNOS activation secondary to caveolin-1 deficiency induces pulmonary hypertension in mice and humans through PKG nitration. *J Clin Invest*. 2009;119(7):2009–18.
46. Schwiening M, Swietlik EM, Pandya D, Burling K, Barker P, Feng OY, Treacy CM, Abreu S, Wort SJ, Pepke-Zaba J, Graf S, Marciniak SJ, Morrell NW, Soon E. Different cytokine patterns in BMPR2-mutation-positive patients and patients with pulmonary arterial hypertension without mutations and their influence on survival. *Chest*. 2022;161(6):1651–6.
47. Rafikov R, Rischard F, Vasilyev M, Varghese MV, Yuan JXJ, Desai AA, Garcia JGN, Rafikova O. Cytokine profiling in pulmonary arterial hypertension: the role of redox homeostasis and sex. *Transl Res*. 2022;247:1–18.
48. Ranchoux B, Antigny F, Rucker-Martin C, Hautefort A, P  choux C, Bogaard HJ, Dorfmu  ller P, Remy S, Lecerf F, Plant   S, Chat S, Fadel E, Houssaini A, Anegon I, Adnot S, Simonneau G, Humbert M, Cohen-Kaminsky S, Perros F. Endothelial-to-mesenchymal transition in pulmonary hypertension. *Circulation*. 2015;131(11):1006–18.
49. Long L, Crosby A, Yang X, Southwood M, Upton PD, Kim DK, Morrell NW. Altered bone morphogenetic protein and transforming growth factor- β signaling in rat models of pulmonary hypertension: potential for activin receptor-like kinase-5 inhibition in prevention and progression of disease. *Circulation*. 2009;119(4):566–76.
50. Igarashi J, Shoji K, Hashimoto T, Moriue T, Yoneda K, Takamura T, Yamashita T, Kubota Y, Kosaka H. Transforming growth factor- β 1 downregulates caveolin-1 expression and enhances sphingosine 1-phosphate signaling in cultured vascular endothelial cells. *Am J Physiol Cell Physiol*. 2009;297(5):C1263–74.
51. Stankevicius E, Kevelaitis E, Vainorius E, Simonsen U. [Role of nitric oxide and other endothelium-derived factors]. *Medicina (Kaunas)*. 2003;39(4):333–41.
52. Ramzy D, Rao V, Tumiaty LC, Xu N, Sheshgiri R, Miriuka S, Delgado DH, Ross HJ. Elevated endothelin-1 levels impair nitric oxide homeostasis through a PKC-dependent pathway. *Circulation*. 2006;114:114.

SUPPORTING INFORMATION

Additional supporting information can be found online in the Supporting Information section at the end of this article.

How to cite this article: Erewele EO, Castellon M, Loya O, Marshboom G, Schwartz A, Yerlioglu K, Callahan C, Chen J, Minshall RD, Oliveira SD. Hypoxia-induced pulmonary hypertension upregulates eNOS and TGF- β contributing to sex-linked differences in *BMPR2*^{+ / R899X} mutant mice. *Pulm Circ*. 2022;e12163.
<https://doi.org/10.1002/pul2.12163>